

## Application of Nickel-Alginate Beads in Reducing Methylene Blue Contamination in Aqueous Media

Azwinda Qonita Yusry<sup>1</sup>, Tien Setyaningtyas<sup>1</sup>, Kapti Riyani<sup>1</sup>, Alin Amaliana Sulistyowati<sup>1</sup>, Anung Riapanitra<sup>1\*</sup>

<sup>1</sup>Department of Chemistry, Faculty of Mathematics and Natural Science, Jenderal Soedirman University, Purwokerto, Central Java, 53122, Indonesia

\*Corresponding author: anung.riapanitra@unsoed.ac.id

### Abstract

In this study, Ni-alginate beads (Ni-ABs) were prepared to enhance their adsorption capacity for methylene blue. The adsorbent was characterized using FTIR and SEM instruments. The adsorption of Ni-ABs for methylene blue was investigated in a batch adsorption study. The adsorption conditions for Ni-ABs for methylene blue were optimized, including the pH of the methylene blue solution and contact time. The adsorption capacity of Ni-ABs for methylene blue reached 90% at pH 6 after 90 minutes of contact. The experimental results were evaluated using the Langmuir and the Freundlich isotherm models. The adsorption behavior followed the Freundlich model, suggesting multilayer adsorption. Regeneration of Ni-ABs was successfully performed using a 0.5 M HCl solution. The Ni-ABs exhibited good stability, with adsorption efficiencies ranging from 76–90% and desorption rates between 64–85% over five cycles. These results indicated that Ni-ABs were effective and reusable adsorbents for the selective removal of methylene blue from aqueous solutions. This study demonstrates a simple Ni-alginate bead system with high reusability as a low-cost alternative adsorbent compared to previously reported alginate-based materials.

### Keywords

Nickel-Alginate Beads, Adsorption, Methylene Blue, Regeneration, Dye Removal

Received: 23 November 2025, Accepted: 26 January 2026

<https://doi.org/10.26554/ijmr.20264177>

## 1. INTRODUCTION

Methylene blue is a synthetic dye classified as an aromatic hydrocarbon compound that possesses toxic properties. Furthermore, it is a cationic dye with a robust adsorption capacity. This colorant has extensive application across various sectors, including the textile, food, paper, and leather industries (Al-Asadi et al., 2025; El Hassani et al., 2022). When persistent in the environment, this compound is challenging to biodegrade, subsequently posing health risks due to its carcinogenic and mutagenic nature. Exposure to MB can induce cyanosis upon inhalation and cause skin irritation upon dermal contact (Khan et al., 2022; Umesh et al., 2024).

Adsorption stands out as one of the superior methodologies for mitigating dissolved organic pollutants, such as those derived from textile industry dye effluents. This technique plays a vital role in environmental remediation efforts concerning dye wastewater contamination. Its effectiveness is attributed to several advantages: it is straightforward to execute, demonstrates a high success rate, and requires low operational costs. Fundamentally, adsorption occurs at the surface of a solid material due to attractive forces between the atoms or molecules of that solid (Cai et al., 2025).

Recent studies have demonstrated that advanced adsorption

materials such as biochar-based composites, polymer-inorganic hybrids, and functional hydrogels exhibit enhanced dye removal efficiency due to improved surface chemistry and tunable pore (Abdulhameed et al., 2025; Chen et al., 2025; Ramadhan et al., 2025; Younis et al., 2025). In particular, adsorption materials derived from sustainable resources have gained increasing attention because they combine high removal efficiency with environmental compatibility and low production cost (Putri et al., 2025). These developments highlight the growing need for simple, reusable, and eco-friendly adsorbents capable of treating dye-contaminated wastewater under mild conditions.

Alginate is a naturally occurring anionic polymer derived from brown seaweed. Chemically, it is a linear copolymer comprising  $\beta$ -D-mannuronate (1,4)-linked units and  $\alpha$ -L-guluronate units. Alginate possesses several desirable characteristics, including biocompatibility, biodegradability, low toxicity, and cost-effectiveness (Jadach et al., 2022; Zhang et al., 2023). In recent years, alginate-based hydrogels and bead-type adsorbents have emerged as promising materials for wastewater treatment because of their high swelling capacity, abundant functional groups, and ease of recovery from treated solutions (Chen et al., 2025). The composites provide enhanced mechanical strength and enable mild gelation with the addition of divalent or trivalent

cations. The bead morphology is a valuable alternative form that can significantly improve the material's swelling capacity (Wu et al., 2024).

The incorporation of metal ions, carbon materials, or inorganic fillers into alginate matrices has been reported to significantly enhance adsorption performance, mechanical stability, and reusability, making these systems attractive for practical water treatment applications (Hao et al., 2025; Joolaei Ahranjani et al., 2025; Kousar et al., 2025). Extensive research has focused on the use of alginate beads as effective adsorbents. Various metal-alginate gel beads, including Sr-alginate, Co-alginate, Ca-alginate, and Ni-alginate, have been synthesized for the removal of heavy metals. Their findings indicated that Ni-alginate gel beads exhibited superior lead ion removal capacity compared to other metal-alginate beads, achieving a 93.3% removal efficiency (Sami et al., 2022). However, most previous studies on Ni-alginate beads have focused on heavy metal ions remediation, while their application for organic dye removal and reusability have been rarely reported. In addition, the regeneration performance of Ni-alginate systems remains poorly understood. Based on these compelling previous studies, the current research intends to synthesize Ni-alginate gel beads (Ni-ABs). This material will subsequently undergo characterization and be applied as an adsorbent for the removal of methylene blue dye. Therefore, this research aimed to develop Ni-alginate gel beads as an adsorbent with a higher adsorption capacity and excellent ease of separation from the contaminated sample solution. This study hypothesizes that nickel-alginate beads can serve as an efficient, reusable adsorbent for the removal of methylene blue from aqueous solutions. Specifically, it is hypothesized that  $\text{Ni}^{2+}$  crosslinking enhances bead structural stability, increases the availability of active adsorption sites, and improves adsorption efficiency and regeneration performance compared to conventional alginate beads.

## 2. EXPERIMENTAL

### 2.1 Materials

Materials used in this experiment were sodium alginate, calcium chloride ( $\text{CaCl}_2$ ) (Merck), nickel(II) chloride hexahydrate ( $\text{NiCl}_2 \cdot 6\text{H}_2\text{O}$ ) (Merck), Methylene blue (MB) (Merck), Hydrochloric acid (HCl) (Merck), and sodium hydroxide (NaOH) (Merck). Demineralized and deionized water were used throughout all experimental procedures, including solution preparation, washing, and bead storage. All chemicals were of analytical reagent grade and were used as received without further purification. The characterization of the samples was performed using a Shimadzu IRTracer-100 Fourier Transform Infrared Spectrometer (FTIR) to identify the functional groups present and a JEOL JSM-6520LA Scanning Electron Microscope (SEM) to assess the surface morphology. The absorbance of the samples were measured using a Shimadzu 1800 UV-Visible spectrophotometer.

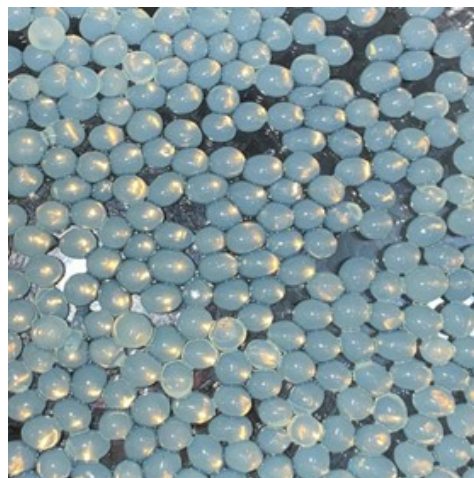


Figure 1. Alginate Beads with The Addition of  $\text{Ni}^{2+}$

## 2.2 Methods

### 2.2.1 Ni-ABs Synthesis

A 2% (w/v) sodium alginate solution was prepared and stirred with a magnetic stirrer for 2 hours to achieve complete homogenization. This homogeneous solution was subsequently added dropwise to a hardening solution. The hardening solution consisted of 0.15 M  $\text{CaCl}_2$  and 0.05 M  $\text{NiCl}_2 \cdot 6\text{H}_2\text{O}$ . Nickel-modified alginate beads (Ni-ABs) formed immediately upon contact. The resulting mixture was continuously stirred for two hours. Following this stirring period, the Ni-ABs were filtered, rinsed twice with demineralized water, and then immersed in fresh deionized water. The prepared Ni-ABs were stored at refrigerated temperatures (1-4 °C).

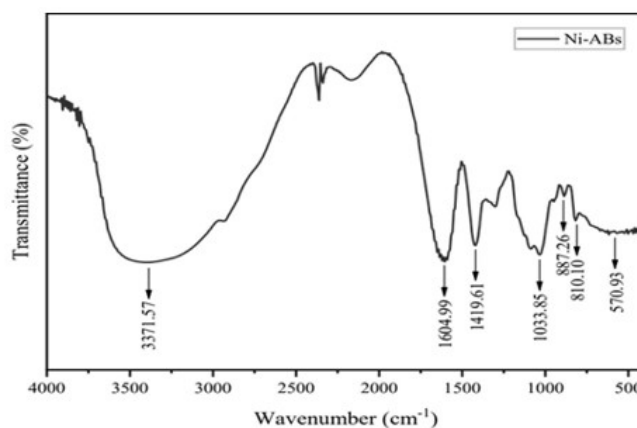


Figure 2. FTIR Characterization Results of Ni-ABs

### 2.2.2 pH Variation

3 grams of Ni-ABs were added to 20 mL of a 10 ppm methylene blue solution. The pH of these solutions was systematically varied to 3, 4, 5, 6, 7, and 8, adjusted with 0.01 M NaOH or 0.01 M HCl. The mixture was agitated in a shaker for 1 hour.

Subsequently, the solutions were analyzed to determine the final methylene blue concentration by measuring their absorbance at 664 nm using a UV-Visible spectrophotometer (Hellal et al., 2023).

### 2.2.3 Contact Time Variation

3 grams of Ni-ABs were combined with 20 mL of a 10 ppm methylene blue solution maintained at the previously determined optimum pH. The mixtures were then agitated using a shaker at 0, 30, 60, 90, 120, 150, and 180 minutes. After each contact period, the residual methylene blue concentration was quantified by measuring the solution's absorbance at its maximum wavelength utilizing a UV-Visible spectrophotometer (Hellal et al., 2023).

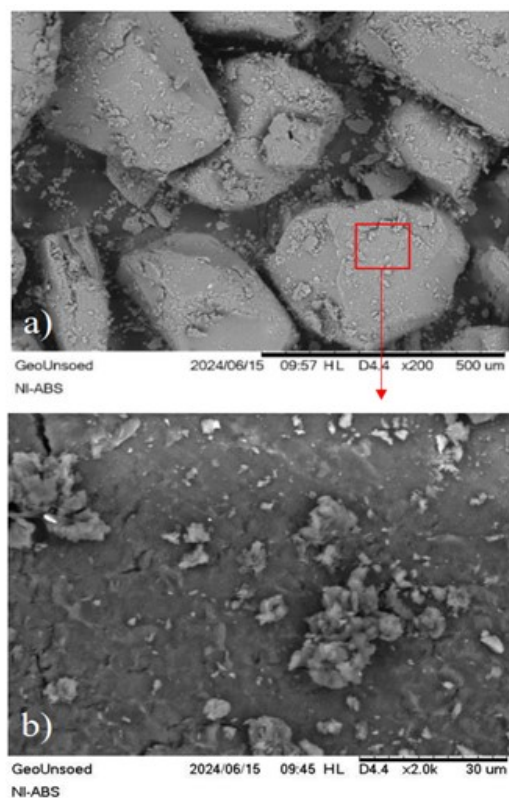


**Figure 3.** Characterization Results of Ni-ABs Using SEM at (a) 200× Magnification; and (b) 2000× Magnification

### 2.2.4 Isotherm Models Evaluation

5 grams of Ni-ABs were exposed to 20 mL of a 10 ppm methylene blue solution at various initial concentrations (10, 20, 30, 40, 50, and 100 ppm), all maintained at the optimum pH. Agitation of these suspensions was subsequently performed using a shaker for the previously determined optimum contact time. Following the adsorption process, the final residual concentration was determined by measuring the solution's absorbance at the maximum wavelength using a UV-Visible spectrophotometer (Hellal et al., 2023).

### 2.2.5 Regeneration Test of Ni-ABs

The regeneration and reusability study commenced by treating a 10 ppm methylene blue solution with 5 grams of Ni-ABs at the optimum pH. The mixture was agitated in a shaker at room temperature for the optimal contact time. Following the adsorption step, the adsorbent was separated from the solution and filtered. The resulting filtrate was analyzed by measuring its absorbance at the maximum wavelength using a UV-Visible spectrophotometer, while the recovered adsorbent was subsequently dried. For the desorption phase, the dried adsorbent was immersed in 20 mL of 0.5 M HCl and agitated using a shaker for 30 minutes. The solution was then filtered, and the filtrate (containing the desorbed dye) was analyzed by measuring its absorbance at the maximum wavelength using a UV-Visible spectrophotometer. The recovered adsorbent was again dried and washed with demineralized water. This entire adsorption-desorption-washing cycle was repeated for a total of five consecutive cycles (Blanco et al., 2023).

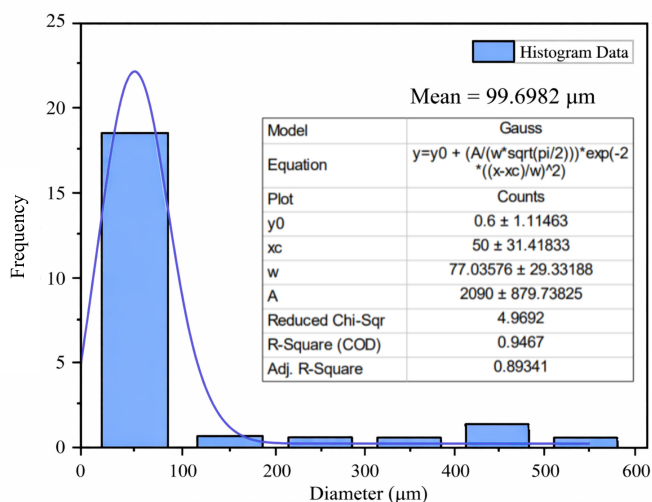


**Figure 4.** Particle Size Distribution Derived from SEM Analysis

## 3. RESULTS AND DISCUSSION

### 3.0.1 Ni-ABs Synthesis

The Ni-ABs have been successfully synthesized using the simple dripping method (extrusion), as presented in Figure 1. This method involves the dropwise extrusion of the alginate from a syringe into a hardening solution. As the alginate solution exits the syringe, droplets form at the needle tip. The droplets are fully formed when they reach a size that allows them to detach from the syringe tip and fall into the hardening solution. Subsequently, the alginate droplets form spheres due to the liquid surface tension (Lin et al., 2024).

The Ni-ABs exhibited a light green color, which originates from the Ni<sup>2+</sup> added as the hardening solution. The Ca<sup>2+</sup> hardening solution was combined with Ni<sup>2+</sup>, to promote a more compact gel network in the alginate compared to using only Ca<sup>2+</sup> (Ramdhan et al., 2022).

### 3.0.2 Characterization of Ni-ABs

Based on Figure 2, the Ni-ABs adsorbent confirmed the successful synthesis and the structural integrity of the alginate-nickel complex. The spectrum revealed a characteristic broad and strong absorption band at  $3371.57\text{ cm}^{-1}$ , indicative of the O–H stretching vibration inherent to the alginate structure. Crucially, the presence of the alginate polymer was established by the characteristic absorption in the carboxylate group region C=O asymmetric stretch at  $1604.99\text{ cm}^{-1}$  and symmetric stretch at  $1419.61\text{ cm}^{-1}$ , confirming that the carboxylate groups  $-\text{COO}^-$  serve as the primary active adsorption sites. Furthermore, the successful incorporation of the cross-linking agent was evidenced by a distinct peak at  $570.93\text{ cm}^{-1}$ , attributed to the Ni–O bond, thus confirming the ionotropic cross-linking mechanism and the formation of the Ni-ABs adsorbent (Liu et al., 2022). The appearance of the Ni–O vibration band at  $570.93\text{ cm}^{-1}$  confirms the successful crosslinking of alginate chains by  $\text{Ni}^{2+}$  ions, forming a stable three-dimensional network. This crosslinked structure not only improves the mechanical stability of the beads but also creates accessible adsorption sites within the gel matrix, facilitating diffusion and binding of methylene blue molecules. Therefore, the adsorption mechanism of methylene blue onto Ni-ABs is primarily governed by electrostatic interactions between  $-\text{COO}^-$  groups and MB cations, supported by hydrogen bonding with  $-\text{OH}$  groups.

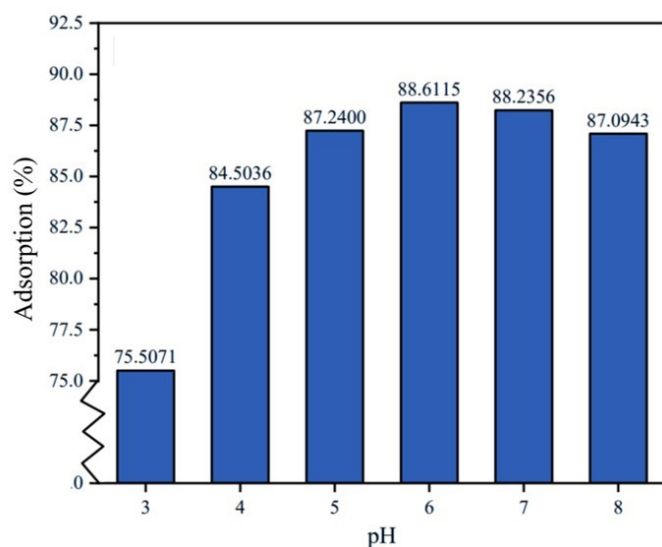


**Figure 5.** The Effect of pH Variation on the Percentage of Methylene Blue Dye Adsorption

Based on Figure 3 (a), the SEM analysis at  $200\times$  magnification revealed that the Ni-ABs exhibited an amorphous, flake-like morphology (irregular shape) characterized by a highly compact surface interspersed with several cracks. Further examination at  $2000\times$  magnification as shown in Figure 3 (b), provided a detailed view. The image reveal that the Ni-ABs had a rough, uneven surface texture, organized into granules with numerous wrinkles and pores. This high degree of surface irregularity is beneficial

for the material's adsorbent function. An average particle size of  $99.6982\text{ }\mu\text{m}$  was observed for the synthesized Ni-ABs thereby demonstrating the achievement of micro-scale synthesis as presented in Figure ???. The data distribution ( $n=25$ ) extended from  $4.243$  to  $507.137\text{ }\mu\text{m}$ , with a dominant cluster ( $n=18$ ) in the  $0\text{--}100\text{ }\mu\text{m}$  range, thereby demonstrating the achievement of micro-scale synthesis. The synthesis method for alginate-based gel beads is a determinant factor for particle size, which may vary from nano to micro-dimensions. The extrusion encapsulation method, in particular, produces micro-sized particles (microcapsules) typically within the  $100\text{ nm}$  to  $1000\text{ }\mu\text{m}$  range (Łętocha et al., 2022).

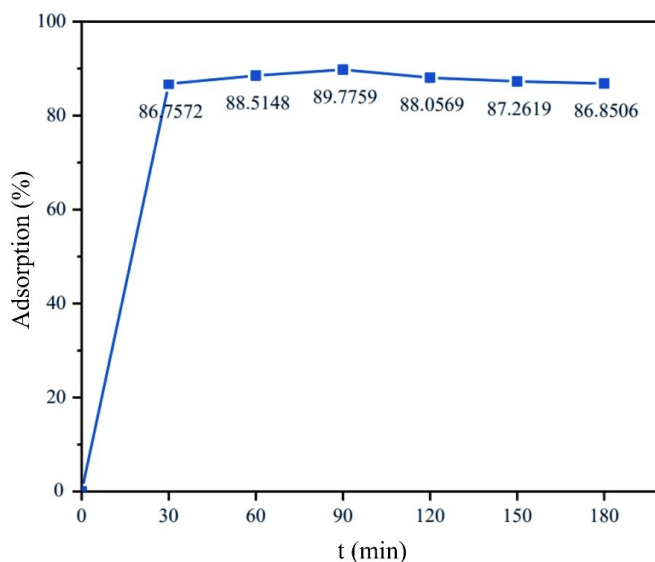


**Figure 6.** The Effect of Variations in Contact Time on the Adsorption Percentage of Methylene Blue

The presence of cracks on the adsorbent surface is attributed to the heterogeneous structural composition of alginate, which typically features a dense surface layer and a loose, less compact core. This structural disparity results in a fragile adsorbent network that is susceptible to damage, particularly during the drying process (Zhang et al., 2019). The compact yet crosslinked structure formed by  $\text{Ca}^{2+}/\text{Ni}^{2+}$  ions contributes to the mechanical stability of the beads, which is essential for maintaining adsorption performance over multiple regeneration cycles. Thus, the SEM analysis confirms that the rough, porous, and cracked morphology of Ni-ABs directly supports their high adsorption capacity and good reusability, as observed in the adsorption and regeneration experiments.

### 3.1 Adsorption

Figure 5 indicates that the adsorption percentage increased significantly as the pH was raised from 3 to 6, achieving the optimum removal efficiency at pH 6. This dependence is explained by the influence of pH on the adsorbent's surface charge: at  $\text{pH} < 6$ , the excess  $\text{H}^+$  ions cause protonation of the  $-\text{OH}$  and  $\text{C}=\text{O}$  active

sites on the Ni-ABs surface. This protonation reduces the negative charge and increases the positive charge density, leading to electrostatic repulsion between the positively charged methylene blue cations and the adsorbent, thus hindering adsorption and resulting in low removal rates. Conversely, the condition at pH 6 establishes charge equilibrium, minimizing competitive  $H^+$  effects and allowing maximal interaction between the partial positive charge of methylene blue and the available active sites on the Ni-ABs surface (Joolaei Ahranjani et al., 2025).

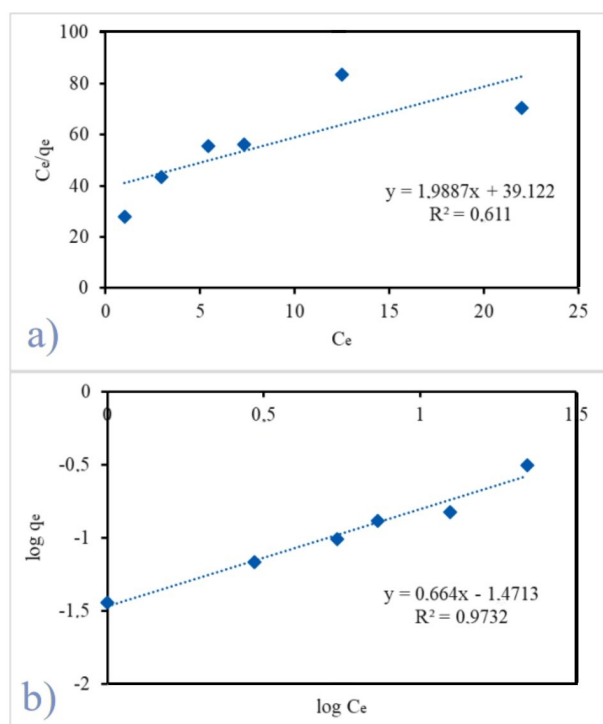


**Figure 7.** Adsorption Isotherm Models (a) Langmuir Isotherm, and (b) Freundlich Isotherm for Ni-ABs Adsorbent

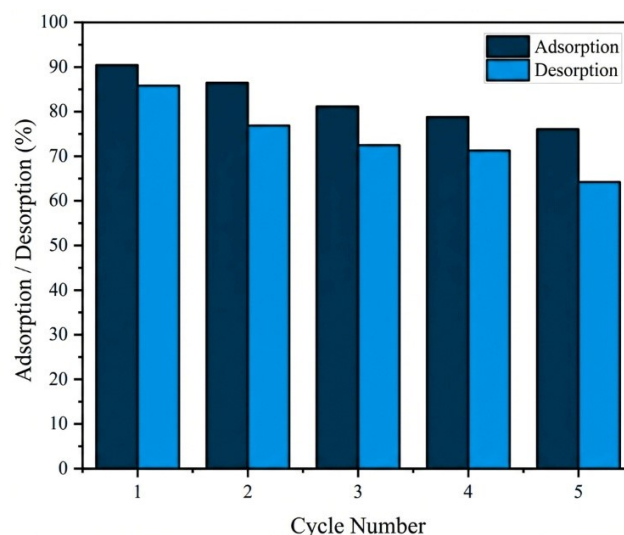
The decrease in adsorption percentage observed beyond the optimum pH is primarily due to two factors: saturation of the adsorbent's active sites and the formation of precipitates that interfere with adsorption. Furthermore, at high pH, methylene blue ions exist predominantly in zwitterionic form, which significantly promotes molecular aggregation into larger species, specifically dimers. This increase in molecular size makes it substantially more difficult for the dye to enter the adsorbent pores. The formation of these larger aggregates of the methylene blue zwitterions is driven by electrostatic attractive interactions between the ionic groups of the zwitterion and its monomers (Sari Yilmaz, 2022; Shi et al., 2022).

Figure 6 shows that the adsorption percentage increased steadily from 30 minutes to 60 minutes, then continued to rise until the optimum contact time of 90 minutes was reached. This initial rapid uptake is attributed to the large number of vacant active sites on the adsorbent surface, facilitating abundant interaction between the adsorbent and the adsorbate (Dimbo et al.,

2024; Loutfi et al., 2023). At the optimum time of 90 minutes, the highest adsorption percentage obtained was 89.79%. Consequently, this contact time was adopted for the subsequent experimental procedures in this study.

Beyond the optimal contact time, extending the contact period between the adsorbent and the adsorbate did not yield a significant increase in dye removal. This effect occurs because most of the active sites on the adsorbent surface have become occupied by methylene blue molecules, causing the adsorption rate to significantly decrease due to the limited availability of remaining vacant binding sites (Samadi Kazemi and Sobhani, 2023).

Based on the analysis of adsorption isotherms for methylene blue on Ni-ABs, the most suitable model was determined by evaluating the coefficient of determination ( $R^2$ ). A value of  $R^2$  approaching 1 signifies a strong correlation and interdependence among the variables, thus indicating the most appropriate isotherm model (Allahkarami et al., 2024). The linear regression results showed that the  $R^2$  value for the Langmuir isotherm model in shown Figure 7(a) was 0.6110, while the  $R^2$  value for the Freundlich isotherm model shown in Figure 7(b) was 0.9732. Following the principle that the isotherm model with the highest coefficient of determination is the most representative, it is concluded that the adsorption process of methylene blue dye by the Ni-ABs adsorbent obeys the Freundlich adsorption isotherm model (Liu et al., 2023).



**Figure 8.** Regeneration Test of Ni-ABs

Figure 8 illustrates a gradual decrease in the methylene blue adsorption percentage across successive cycles, a trend likely influenced by the desorption process's efficiency. The highest desorption percentage was recorded in the first cycle, reaching 85.84%. This high efficiency is attributed to the mechanism of the HCl desorbing agent:  $H^+$  ions strongly interact with the adsorbent surface, effectively competing with and displacing the already bound methylene blue cations back into the solution,

due to the  $H^+$  ions' robust bonding affinity (Buelvas et al., 2023). Conversely, the lowest desorption percentage in the fifth cycle, 64.24% suggests that the active groups on the adsorbent surface became less susceptible to protonation, making it increasingly difficult for the methylene blue ions to detach (Ivanets et al., 2022). The sub-optimal desorption efficiency meant that residual adsorbate remained on the surface, thereby reducing the number of available active sites for the next adsorption cycle, leading to the observed decrease in subsequent adsorption percentages. However, this overall decline was not overly significant, indicating the Ni-ABs possessed good stability and remained effective over five usage cycles, as the final adsorption percentage remained above 60%, confirming good reusability (Tohdee et al., 2024). These results confirm that methylene blue adsorption by Ni-ABs is dominated by electrostatic attraction and hydrogen bonding, as previously indicated by FTIR analysis and pH-dependent adsorption behavior.

#### 4. CONCLUSIONS

Ni-alginate gel beads (Ni-ABs) have been successfully synthesized using the simple dripping method, yielding light-green gel beads. Ni-alginate gel beads have good stability with an adsorption range of 76-90% in five repetitions. The adsorption of methylene blue by Ni-alginate gel beads was optimal at pH 6 and a contact time of 90 minutes, with an adsorption percentage of 90%. The adsorption isotherm data were best fitted to the Freundlich Isotherm model. These findings confirm the proposed hypothesis that  $Ni^{2+}$  crosslinking enhances structural stability, active site availability, and reusability of alginate beads for dye adsorption. Future studies should focus on investigating the adsorption kinetics and thermodynamics of methylene blue removal using Ni-alginate beads to provide deeper insight into the adsorption mechanism and rate-controlling steps. The performance of Ni-ABs should also be evaluated in real textile wastewater to assess their performance under practical conditions, accounting for competing ions and organic matter. In addition, surface modification of Ni-alginate beads or incorporation of secondary functional materials (such as carbon-based additives or metal oxides) may further enhance adsorption capacity and selectivity. Finally, continuous-flow column studies are recommended to evaluate the scalability and long-term operational stability of the adsorbent for real wastewater treatment applications.

#### 5. ACKNOWLEDGEMENT

The authors gratefully acknowledge that this research was funded by the Inorganic Laboratory research team. The authors also thank the Department of Chemistry, Faculty of Mathematics and Natural Sciences, Jenderal Soedirman University, for providing laboratory facilities and instrumentation support for this study.

#### REFERENCES

Abdulhameed, A. S., S. Abdullah, A. A. Altamimi, M. Abualhaija, and S. Algburi (2025). Hybrid Polymer Nanocomposite of

- Ionically Crosslinked Chitosan/Tin Oxide Nanoparticles for Eosin Y Dye Removal: Isotherm, Kinetic, and Adsorption Optimization. *Journal of Applied Polymer Science*, **142**(43); e57662
- Al-Asadi, S. T., Z. H. Mussa, F. F. Al-Qaim, H. Kamyab, H. F. S. Al-Saedi, I. F. Deyab, and N. J. Kadhim (2025). A Comprehensive Review of Methylene Blue Dye Adsorption on Activated Carbon from Edible Fruit Seeds: A Case Study on Kinetics and Adsorption Models. *Carbon Trends*, **20**; 100507
- Allahkarami, E., E. Allahkarami, M. Heydari, A. Azadmehr, and A. Maghsoudi (2024). Assessment of Chromite Ore Wastes for Methylene Blue Adsorption: Isotherm, Kinetic, Thermodynamic Studies, ANN, and Statistical Physics Modeling. *Chemosphere*, **358**; 142098
- Blanco, L., O. Martínez-Rico, Á. Domínguez, and B. González (2023). Removal of Acid Blue 80 from Aqueous Solutions Using Chitosan-Based Beads Modified with Choline Chloride:Urea Deep Eutectic Solvent and FeO. *Water Resources and Industry*, **29**; 100195
- Buelvas, D. D. A., L. P. Camargo, I. K. I. Salgado, B. L. S. Vicentin, D. F. Valezi, L. H. Dall'Antonia, and E. Di Mauro (2023). Study and Optimization of the Adsorption Process of Methylene Blue Dye in Reusable Polyaniline-Magnetite Composites. *Synthetic Metals*, **292**; 117232
- Cai, F., C. Li, C. Yang, Y. Wang, H. Zhou, S. Yang, and Y. Liu (2025). Preparation of Nitrogen-Doped Bagasse-Derived Biochar with Outstanding Methylene Blue Adsorption Performance. *Industrial Crops and Products*, **224**; 120415
- Chen, M., A. Long, W. Zhang, Z. Wang, X. Xiao, Y. Gao, and H. Wang (2025). Recent Advances in Alginate-Based Hydrogels for the Adsorption-Desorption of Heavy Metal Ions from Water: A Review. *Separation and Purification Technology*, **353**; 128265
- Dimbo, D., M. Abewaa, E. Adino, A. Mengistu, T. Takele, A. Oro, and M. Rangaraju (2024). Methylene Blue Adsorption from Aqueous Solution Using Activated Carbon of *Spathodea campanulata*. *Results in Engineering*, **21**; 101910
- El Hassani, S. E. A., A. Driouch, H. Chaair, H. Mellouk, and K. Digua (2022). Optimization of Activated Carbon by Chemical Activation from Grape Seeds Using the Response Surface Methodology. *Desalination and Water Treatment*, **245**; 144–157
- Hao, J., C. Bi, S. Li, S. Zhao, S. Yang, Y. Li, and T. E (2025). Structural Regulation of Alginate-Based Adsorbents Based on Different Coordination Configurations of Metal Ions and Selective Adsorption of Copper Ion. *International Journal of Biological Macromolecules*, **284**; 138160
- Hellal, M. S., A. M. Rashad, K. K. Kadimpati, S. K. Attia, and M. E. Fawzy (2023). Adsorption Characteristics of Nickel (II) from Aqueous Solutions by Zeolite Socony Mobile-5 (ZSM-5) Incorporated in Sodium Alginate Beads. *Scientific Reports*, **13**(1); 19601
- Ivanets, A., V. Prozorovich, M. Roshchina, O. Sychova, V. Srivastava, and M. Sillanpää (2022). Methylene Blue Adsorption on Magnesium Ferrite: Optimization Study, Kinetics and Reusability. *Materials Today Communications*, **31**; 103594

- Jadach, B., W. Świetlik, and A. Froelich (2022). Sodium Alginate as a Pharmaceutical Excipient: Novel Applications of a Well-Known Polymer. *Journal of Pharmaceutical Sciences*, **111**(5); 1250–1261
- Joolaei Ahranjani, P., K. Dehghan, S. Farhoudi, M. Esmaeili Bidhendi, Z. Sotoudehnia Korrani, and S. Rezaia (2025). Effective Removal of Nitrate and Phosphate Ions from Water Using Nickel-Doped Calcium Alginate Beads. *Process Safety and Environmental Protection*, **194**; 486–496
- Khan, I., K. Saeed, I. Zekker, B. Zhang, A. H. Hendi, A. Ahmad, and I. Khan (2022). Review on Methylene Blue: Its Properties, Uses, Toxicity and Photodegradation. *Water*, **14**(2); 242
- Kousar, S., M. Fan, K. Javed, B. Begum, M. M. Naeem, S. Zhang, and X. Hu (2025). Hydrothermal Carbonization of Rice/Sodium Alginate Chelating Metal Chloride with Bead-Like Structures Forms Hydrochar of Distinct Property. *Inorganic Chemistry Communications*, **180**; 114962
- Lin, Y., J. Xu, and X. Gao (2024). Development of Antioxidant Sodium Alginate Gel Beads Encapsulating Curcumin/Gum Arabic/Gelatin Microcapsules. *Food Hydrocolloids*, **152**; 109901
- Liu, C., P. Li, Y. J. Xu, Y. Liu, P. Zhu, and Y. Z. Wang (2022). Bio-Based Nickel Alginate toward Improving Fire Safety and Mechanical Properties of Epoxy Resin. *Polymer Degradation and Stability*, **200**; 109945
- Liu, G., Z. Liu, S. Li, C. Shi, T. Xu, M. Huo, and Y. Lin (2023). Aluminum–Copper Bimetallic Metal Organic Gels/Sodium Alginate Beads for Efficient Adsorption of Ciprofloxacin and Methylene Blue: Adsorption Isotherm, Kinetic and Mechanism Studies. *Process Safety and Environmental Protection*, **176**; 763–775
- Loutfi, M., R. Mariouch, I. Mariouch, M. Belfaquir, and M. S. Elyoubi (2023). Adsorption of Methylene Blue Dye from Aqueous Solutions onto Natural Clay: Equilibrium and Kinetic Studies. *Materials Today: Proceedings*, **72**; 3638–3643
- Łętocha, A., M. Miastkowska, and E. Sikora (2022). Preparation and Characteristics of Alginate Microparticles for Food, Pharmaceutical and Cosmetic Applications. *Polymers*, **14**(18); 3834
- Putri, B. I., F. S. Arsyad, Y. Hanifah, and N. Ahmad (2025). *Eucheuma Cottonii* Hydrochar: A Promising Adsorbent for Congo Red Dye. *Indonesian Journal of Material Research*, **3**(2); 62–71
- Ramadhan, N., A. S. Aliyah, R. J. Sayeri, and N. R. Palapa (2025). A Review on Azo Dyes Removal from Wastewater Using Biochar-Based Adsorbents: Materials, Mechanisms, and Perspectives. *Indonesian Journal of Material Research*, **3**(2); 47–56
- Ramadhan, T., S. Hung Ching, S. Prakash, and B. Bhandari (2022). Evaluation of Alginate-Biopolymers (Protein, Hydrocolloid, Starch) Composite Microgels Prepared by the Spray Aerosol Technique as a Carrier for Green Tea Polyphenols. *Food Chemistry*, **371**; 131382
- Samadi Kazemi, M. and A. Sobhani (2023). CuMn<sub>2</sub>O<sub>4</sub>/Chitosan Micro/Nanocomposite: Green Synthesis, Methylene Blue Removal, and Study of Kinetic Adsorption, Adsorption Isotherm Experiments, Mechanism and Adsorbent Capacity. *Arabian Journal of Chemistry*, **16**(6); 104754
- Sami, N. M., A. A. Elsayed, M. M. S. Ali, and S. S. Metwally (2022). Ni-Alginate Hydrogel Beads for Establishing Breakthrough Curves of Lead Ions Removal from Aqueous Solutions. *Environmental Science and Pollution Research*, **29**(53); 80716–80726
- Sari Yilmaz, M. (2022). Graphene Oxide/Hollow Mesoporous Silica Composite for Selective Adsorption of Methylene Blue. *Microporous and Mesoporous Materials*, **330**; 111570
- Shi, Y., G. Song, A. Li, J. Wang, H. Wang, Y. Sun, and G. Ding (2022). Graphene Oxide–Chitosan Composite Aerogel for Adsorption of Methyl Orange and Methylene Blue: Effect of pH in Single and Binary Systems. *Colloids and Surfaces A: Physicochemical and Engineering Aspects*, **641**; 128595
- Tohdee, K., S. Semmad, A. Jotisanakasa, B. Jongsomjit, T. Somsiripan, and Asadullah (2024). Sustainable Adsorption of Methylene Blue onto Biochar-Based Adsorbents Derived from Oil Palm Empty Fruit Branch: Performance and Reusability Analysis. *Bioresource Technology Reports*, **25**; 101755
- Umesh, A. S., Y. M. Puttaiahgowda, and S. Thottathil (2024). Enhanced Adsorption: Reviewing the Potential of Reinforcing Polymers and Hydrogels with Nanomaterials for Methylene Blue Dye Removal. *Surfaces and Interfaces*, **51**; 104670
- Wu, Z., J. Su, X. Cong, D. Zhao, J. Wu, H. Zhou, and B. Sun (2024). Preparation, Characterization, and Mechanism of Swelling and Cu<sup>2+</sup> Adsorption by Alginate-Based Beads Enhanced with Huangshui Polysaccharides. *Journal of Cleaner Production*, **475**; 143622
- Younis, M. Y., W. Li, J. Khan, and Y. Wei (2025). Lotus Carbon Dots Doped Sodium Alginate Hydrogel Beads for Effective Adsorptive Removal of Cd<sup>2+</sup> and Potential Application in Pb<sup>2+</sup> Removal from Wastewater. *International Journal of Biological Macromolecules*, **322**; 146638
- Zhang, X., X. Lin, H. Ding, Y. He, H. Yang, Y. Chen, and X. Luo (2019). Novel Alginate Particles Decorated with Nickel for Enhancing Ciprofloxacin Removal: Characterization and Mechanism Analysis. *Ecotoxicology and Environmental Safety*, **169**; 392–401
- Zhang, Y., W. Zhao, Z. Lin, Z. Tang, and B. Lin (2023). Carboxymethyl Chitosan/Sodium Alginate Hydrogel Films with Good Biocompatibility and Reproducibility by In Situ Ultra-Fast Crosslinking for Efficient Preservation of Strawberry. *Carbohydrate Polymers*, **316**; 121073